

# AGGREGATION AND DISAGGREGATION OF ERYTHROCYTES IN WHOLE BLOOD: STUDY BY BACKSCATTERING TECHNIQUE

Alexander V. Priezzhev,<sup>†</sup> Olga M. Ryaboshapka,<sup>†</sup> Nikolai N. Firsov,<sup>‡</sup> and Igor V. Sirko<sup>‡</sup>

<sup>†</sup>M. V. Lomonosov Moscow State University, Physics Department, Vorobiovy Gory, Moscow

119899; <sup>‡</sup>Russian State Medical University, Medico-Biological Department, 1 Ostrovitianova, Moscow 117437, Russia

(Paper ODB-001 received Feb. 3, 1998; revised manuscript received Nov. 18, 1998; accepted for publication Nov. 18, 1998.)

## ABSTRACT

The aggregation phenomenon is of great importance for the evaluation of performance of the microcirculation system because of its influence on the blood viscosity at low shear stresses. Some important features and consequences of this phenomenon *in vivo* can be predicted in the *in vitro* experiments using optical methods. These methods are considered to be the most informative and applicable not only for the basic study of the aggregation phenomenon, but also for the diagnosis of a number of diseases and for the monitoring of therapeutic treatment in clinics. Results presented in this paper prove that the backscattering technique allows one to detect different changes of aggregational ability and deformability of erythrocytes and to get reliable and reproducible results distinguishing normal blood and blood with different pathologies. © 1999 Society of Photo-Optical Instrumentation Engineers. [S1083-3668(99)01001-1]

**Keywords** erythrocyte aggregation; disaggregation; whole blood; Couette viscometer; backscattering.

## 1 INTRODUCTION

When suspended in solution of macromolecules red blood cells (RBCs) have a tendency toward reversible aggregation. Primary aggregates comprising only two adjacent cells develop further into linear aggregates (rouleaux) of different lengths. End-to-side connections of the latter turn them into a three-dimensional (3-D) network that is tightened by cohesive forces into large dense aggregates separated by plasma layers.

It is commonly accepted<sup>1</sup> that such aggregation is mostly due to the nonspecific adsorption of the aggregating plasma proteins on the surfaces of adjacent RBCs. The experiments with different kinds of aggregating proteins showed that there is linear dependence between the velocity of aggregation and the concentration of proteins, temperature, and the deformability of RBCs.<sup>2</sup> In addition, different kinds of plasma proteins induce the formation of different types of aggregates: "clumps" or "networks."<sup>1</sup> Nonetheless there is evidence that protein adsorption is not the only mechanism of aggregation.<sup>3,4</sup>

The morphology of RBC aggregation in whole blood and in RBC suspensions at rest and in shear flow is successfully studied by optical methods. The photometric studies of blood aggregation characteristics were started by the works of Dognon et al.<sup>5,6</sup> who registered the deviation of the intensity of

light scattered from a layer of blood under mixing and after its halt. They have shown the dependence of the signal (scattering intensity) on orientational aggregation of the erythrocytes.

In accord with the primary experiments two approaches have been developed in the aggregometry. The first is based on the registration of light transmission through the studied blood layer in a cone-plate type viscometer.<sup>7,8</sup> It is generally known that aggregation starts with the formation of pairs from which the rouleaux of different lengths are then formed.<sup>2,7,9</sup> These rouleaux are bound "end-to-end" and "end-to side" and form a 3-D network or clumps. Such aggregates containing thousands of erythrocytes are separated one from another by thick layers of plasma.<sup>10</sup> This stage of aggregation is impossible in blood layers as thin as those of the order of 25  $\mu\text{m}$  which is typical of those sites of "cone-plate" aggregometers where the photometry is usually carried out.

In the cone-plate aggregometer the aggregation process reaches the stage of a 2-D network of rouleaux. This is manifested by the characteristic times of the aggregation process calculated from the exponentially decreasing scattering intensity and photocurrent. For example, after the halt of the flow the half-period of the single-exponential aggregation process in normal blood is around  $3.5 \pm 1.0$  s (Ref. 8) while the majority of studies<sup>10,11</sup> have shown that

Address all correspondence to A. V. Priezzhev. Tel: 095-939-2612; Fax: 095-939-3113; E-mail: avp@lbp.ilc.msu.ru

1083-3668/99/\$10.00 © 1999 SPIE

the aggregation process in a stationary suspension preceding the sedimentation continues for 2–3 min. The 50% decrease in amplitude of the signal with respect to the full aggregation amplitude does not describe the morphological changes of the aggregates during the aggregation process.

The second approach is based on the registration of the backscattered light from a blood layer in a Couette type viscometer.<sup>12–14</sup> The commercial apparatuses are the erythroaggregometer Sefam<sup>12,14</sup> and the laser-assisted optical rotational cell analyzer (LORCA).<sup>13</sup> The latter instrument allows interpreting the aggregation phenomenon in terms of kinetics, structural, and rheological parameters. These parameters were found to be sensitive to some pathologies as well as to variations in temperature, hematocrit, and other factors, but they are determined phenomenologically and are not related to the real processes of aggregation and disaggregation. In the LORCA device measurements of the aggregation kinetics are performed on a 0.3 mm wide layer. This condition may be incorrect in some cases such as the hyperaggregation syndrome that is typical of a number of severe hemorheological disorders. The authors also suggest using a parameter such as the half-time of the aggregation kinetics as a quantitative parameter for the diagnosis of oxygenation, anticoagulant, and incubation time effects on the erythrocyte aggregation process.

The diagrams of He-Ne laser light intensities backscattered and transmitted by a concentrated suspension of RBCs in the Couette flow have shapes closely related to the state of the suspension (at rest or subjected to a simple shear flow). An asymmetry in diagrams of backscattered light, absent in the diagrams of transmitted light, is observed when the suspension is in shear flow. This asymmetry is related to the deformation and orientation of the erythrocytes.<sup>15–17</sup>

The backscattered intensity from large structural aggregates is highly sensitive to the changes in their sizes and concentration. Moreover, the use of the backscattering regime is expedient because no moving parts of the device remain in the way of the light beams going into or out of the blood layer.

The goal of our study is to substantiate both experimentally and clinically the efficiency and the advantages of the method of determination of the aggregational properties of whole blood *in vitro* based on registration of the kinetics of backscattering intensity from a thick (1 mm) layer of blood. The aim of this paper is to summarize our experience in this field and to present some basic results, part of which has already been published.<sup>18–24</sup>

## 2 MATERIALS AND METHOD

### 2.1 ERYTHRONEPHELOMETER

The optical scheme of our experimental setup is shown in Figure 1. The sample of blood is placed into a Couette chamber—a 1 mm gap between two

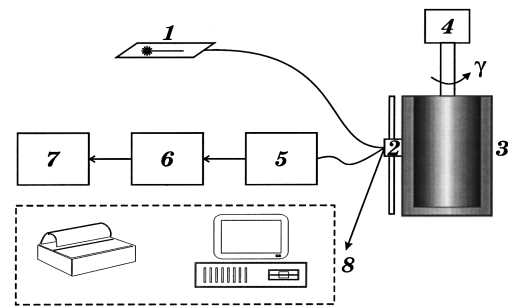


**Fig. 1** Experimental setup of the aggregometer: 1—He-Ne laser, 2—the probing unit, 3—Couette chamber, 4—the motor drive with reductor, 5—photodiode, 6—amplifier, 7—plotting device, 8—computer processing unit.

coaxial cylinders. The outer cylinder is transparent and stationary, whereas the inner one is blackened and can be rotated. The shear rate, which is constant all through the gap except maybe close to the vicinity of the cylinders and the bottom of the couette, can be varied and increased stepwisely. The radiation from a He-Ne or a diode laser in the red light spectrum range (power density 3 mW/mm<sup>2</sup>) is used for probing. The probing unit, basically a light guide 2 mm in diameter, is coupled with four detecting fibers of similar diameter, placed so that the backscattered light can be registered from two pairs of sites located either along or across the direction of the flow. In this respect our setup is considerably different from other systems described, e.g., see Ref. 25. All detected light is fed to a photodiode. The alteration of the intensity of the backscattered light, and consequently, of the photocurrent with time related to the aggregation kinetics, is registered by a plotter or digitized and processed by a computer.

The registration time for one aggregation kinetics from the state of full disaggregation to the state of full aggregation takes about 100–120 s. Complete testing of one blood sample including the registration of one aggregation kinetics and one stepwise disaggregation kinetics takes about 10–15 min.

The process of spontaneous aggregation of RBCs in stasis and aggregates destruction under shear stress are usually represented as dependencies of the backscattered light intensity (remission) on time (in the case of aggregation) or on shear rate (in the case of disaggregation). A typical example of the aggregation kinetics is presented in Figure 2.

### 2.2 BLOOD SAMPLE PREPARATION

Blood drawn from an elbow vein of a donor was put into a glass test tube and stabilized with EDTA solution (0.3 ml of 7% EDTA solution for 10 ml of fresh blood) to prevent clotting. Measurements were usually performed within 6 h after drawing, although the RBCs, when kept in thermostabilized conditions (4–6 °C) in EDTA stabilized autologous plasma, keep their properties for about 30 h with-

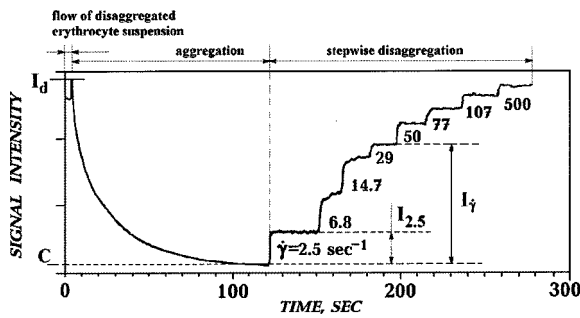


**Fig. 2** The kinetics of spontaneous aggregation and disaggregation of erythrocytes in a sample of whole blood drawn from a healthy donor and measured parameters derived from the aggregation and disaggregation kinetics. Here  $I_d$  is the intensity of backscattered light at the state of total disaggregation,  $I_\gamma$  is that at shear rate  $\dot{\gamma}$ ,  $I_{2.5}$  is that at the shear rate  $\dot{\gamma}=2.5 \text{ s}^{-1}$ . Numbers designate the values of shear rate fixed during the stepwise disaggregation process.

out an alteration of their discoid form and aggregation properties. Before the experiment the volume concentration of erythrocytes (hematocrit) in the sample was measured by means of centrifugation in a capillary tube. The hematocrit values in all studied blood samples ranged from 0.4 to 0.44. The RBC's shape was visually controlled by microscopic observations.

**2.3 EXPERIMENTAL PROCEDURE**

We shall describe the regular experimental procedure with the help of a diagram presented in Figure 2. A 2.4 ml sample of stabilized blood at room temperature is placed into the gap of the aggregometer with a syringe. Then the sample is subjected to high shear rate (about  $840 \text{ s}^{-1}$ ) to destroy all aggregates to single cells. The corresponding shear stress at typical blood viscosity  $\nu=0.04 \text{ Ps}$  is around  $33.6 \text{ dyn/cm}^2$ . At this shear stress normal RBCs start to deform into stretched discoids and to orient relative to the flow direction.

Then the flow is halted. At this moment we observe an instantaneous increase of the backscattered light intensity that is attributed to the transformation of RBCs to their normal shape. Immediately after that the aggregation process starts, lasting for 100–120 s up to complete aggregation. Photometrically this is manifested by the exponential decrease of the backscattered light intensity until saturation.

After that the disaggregation process induced by the stepwise increase of shear rate is detected. At every shear rate the registration of the signal lasts about 10–60 s to avoid the transitional process. In the experiments with normal blood the corresponding stepwise increase of the backscattered light is observed. It is worth noting that in some cases of pathological blood the scattering signal may become lower at low shear rates than at rest because of the shear-induced aggregation.<sup>18</sup> As for this part of the measurement procedure, the backscattered

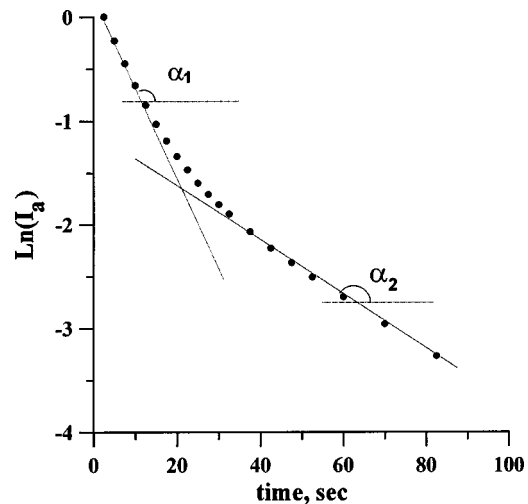


**Fig. 3** The aggregation kinetics in the semilogarithmic scale.  $\alpha_1$  and  $\alpha_2$  are the slope angles of different lines distinguished.

light intensity during the disaggregation process may be subsequently registered at the stepwise increase and decrease of shear rate.

**2.4 SIGNAL PROCESSING AND DATA EVALUATION PROCEDURE**

Now there are some algorithms that are widely used in the aggregometry. The method of exponential expansion of the kinetic curve<sup>13,21</sup> allows us to determine temporal parameters (see below) which are reliably sensitive to different aggregational states of blood and to the effect of physical and chemical factors on blood.<sup>19,20</sup> The method of evaluation of the aggregation rate at a 50% decrease in amplitude of the signal with respect to the full aggregation amplitude<sup>8,13</sup> is also used for the diagnosis of the aggregation properties of erythrocytes.

The representation of the original curve in the semilogarithmic scale (Figure 3) allows us to distinguish two (or in some cases three) lines with different slopes by means of the method of linear regression. Characteristic parameters of these lines are cotangent of the slope angles designated as  $T_1$  and  $T_2$ , corresponding to the subsequent stages of the linear and 3-D aggregates formation. Therefore, phenomenologically the time dependence of the scattering signal intensity  $I_a$  can be described as follows:

$$I_a(t) = Ae^{-(t_1/T_1)} + Be^{-(t-t_1/T_2)} + C.$$

Here  $C$  is the signal intensity at the end of the aggregation process. The digital processing of the signal allows compensating for the  $C$  level, so in Figure 2 the scattering signal designated as 0 really corresponds to the  $C$  level.

The hyperbolic approximation of the original scattering intensity curve allows us to represent  $1/I_a$  as a function of time  $t$  (Figure 4). In this case we

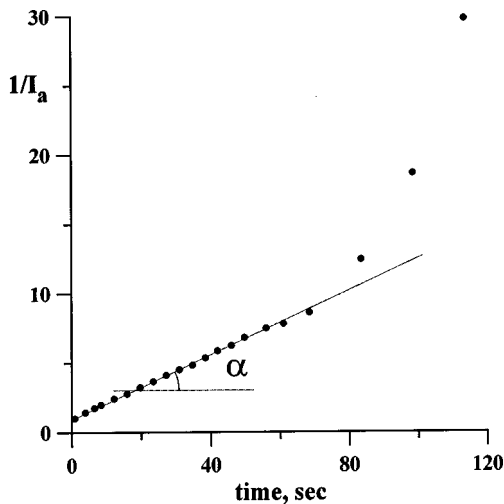


**Fig. 4** The aggregation kinetics presented as a time function of the value  $1/I_a$ .  $\tan \alpha$  determines the rate of the aggregation process in whole.

distinguish only one line, and some points at the end of the aggregation process are placed randomly. This means that the relation

$$I_a \cdot t = \text{const}$$

characterizes the aggregation process as a whole. This parameter is calculated as the tangent of the slope angle ( $\tan \alpha$ ) as shown in Figure 4.<sup>22</sup>

The process of shear-induced disaggregation should be regarded as a relaxational one with approximation of the kinetics by a sum of exponents representing different disaggregation stages. Each of these stages seems to start after the previous one is completed. The shear rate dependence of backscattering intensity is defined as follows:

$$I_d - I_\gamma = Fe^{-(\dot{\gamma}/\beta)},$$

where  $I_d$  is the intensity of backscattered light for complete disaggregation,  $I_\gamma$  is the intensity at shear rate  $\dot{\gamma}$ , and  $\beta$  is the hydrodynamic strength of aggregates. This technique enables reliable determination of a single value of  $\beta$  in the case of normal blood and two different values  $\beta_1$  and  $\beta_2$  in cases of different pathologies.

Thus the basic parameters which we use for the description of the microrheological state of blood are:  $T_1$  is the time of quick aggregation of RBCs and of the linear aggregates formation;  $T_2$  is the time of slow aggregation of RBCs and of the 3D aggregates formation;  $\beta_1$  is the hydrodynamic strength of large aggregates;  $\beta_2$  is the hydrodynamic strength of aggregates;  $I_{2.5}$  is the alteration of backscattered light intensity relative to the state of total aggregation level; and  $\tan \alpha$  is the rate of the aggregation process as a whole. The measured parameters characterize not only the morphology and dimensions of

aggregates but also the kinetics of aggregation. The latter is not restricted to 1-D or 2-D but is extended to 3-D structures.

Measured in different blood preparations (whole blood, whole blood with additives of different polymeric molecules, and washed erythrocytes with additives of different polymeric molecules), these parameters serve much better for the characterization of blood as a complex fluid than mere photographs of the aggregates, and can form a basis for the development of more advanced mathematical models of aggregation. We also measure the deformability of RBCs under shear stress but do not discuss this issue here (see, e.g., Ref. 16).

### 3 RESULTS

During the last few years we have tested more than 1000 samples of blood with the described technique. The experiments with blood samples from healthy donors ( $n=40$ ) showed that the temporal parameters of the aggregation process are:  $T_1 = 12.5 \pm 3.8$  s,  $T_2 = 41.4 \pm 5.1$  s. We found some peculiarities of the aggregation in cases of different pathologies, that are discussed below.

The aggregation process was significantly altered compared to healthy controls both regarding  $T_1$  and  $T_2$  in all diseases studied except for *psoriasis without arthritis*. An increase of  $T_2$  accompanied by the decrease of  $T_1$  compared to healthy controls was found in the blood of patients with *chronic glomerulonephritis* with and without *nephritic syndrome*, *systemic lupus erythematosus*, and *psoriatic arthritis*. In contrast, these parameters for *psoriasis* patients were not different from those of the healthy controls. An increase of  $T_2$  with normal values of  $T_1$  was found in blood from patients with *pulmonary hypertension* and in preoperative patients with *intestinal tumors* aged above 60 years, while *hereditary hypercholesteremia* is characterized by a decrease of  $T_2$  and a normal value of  $T_1$  parameter. Decreased  $T_1$  complemented with a decrease of  $T_2$  was observed in patients with *coronary disease* with and without *diabetes*. A considerable increase of the spontaneous aggregation rate was observed in the blood of patients with these diseases. The number of patients, values of parameters with their standard deviations and comparison with normal ones for all studied pathologies are presented and discussed in more detail elsewhere.<sup>23</sup>

Figure 5 shows that by combining  $T_1$  and  $T_2$ , the aggregation characteristics of pathological blood can be divided into three diagnostic groups:<sup>23</sup> decreased  $T_1$  and increased  $T_2$  (autoimmune diseases); decreased  $T_1$  and decreased  $T_2$  (ischemic heart diseases); and increased  $T_1$  and increased  $T_2$  (other diseases). The combination of increased  $T_1$  and decreased  $T_2$  was not found. The above stated existence of three diagnostic groups defined according to the values of  $T_1$  and  $T_2$  relative to the norm

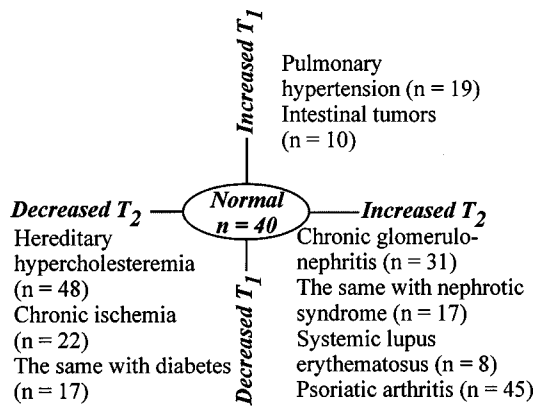


**Fig. 5** Diagram of combination of  $T_1$  and  $T_2$  alterations related to different groups of diseases.

is so far qualitative and is based on the fact that there exists no linear correlation between the above temporal parameters of the aggregation process measured in each sample. Quantitative substantiation of these diagnostic groups needs additional studies with more and various diseases.

The representation of registered aggregation curve in semilogarithmic scale permits us to usually observe two consequential processes of aggregation and a transitional process. The last is related to that state of blood when both linear and primary 3-D aggregates occur. In some cases this part of the whole process comprised 9%–15% of the whole aggregation amplitude and can be also characterized by an additional exponential parameter  $T'_1$ . This parameter is inessential from the viewpoint of diagnostics, but it is supposed to reflect the homogeneity of cohesive properties of erythrocytes. When applying the therapy aimed at the destruction of erythrocyte aggregates by means of dextran DX-40, the transitional process disappears and two characteristic times,  $T_1$  and  $T_2$ , are reliably determined.

The single-exponential process was observed only in the case of *inherited hemoglobinopathy*. This is characterized by a single time parameter with magnitude close to  $T_2$  value. In the case of *inherited hyperlipemia* the spontaneous aggregation process differs from the normal one. The primary aggregation process was found to be of relatively low amplitude but very rapid with characteristic time on the order of 0.5 s (instant aggregation).

We observed the appearance of abnormal kinetics of spontaneous aggregation after plasmapheresis (plasma exchange up to 2 ℓ) performed with patients suffering from *hypercholesterinemia*. The parameter  $T_1$  disappeared and the amplitude of instant process strongly increased up to 50% of the whole aggregation amplitude. Then slow one-exponential aggregation process with characteristic time on the order of  $T_2$  was registered. The transitional process was observed in the shape of a break (Figure 6), a cupola-shaped peak (Figure 7) or a delay of aggregation. Such a delay of the aggregation

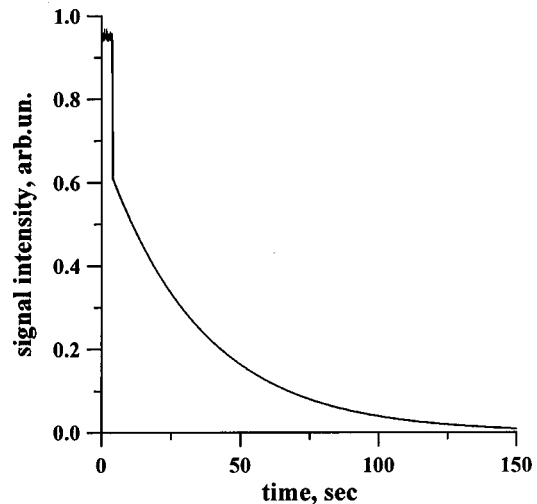


**Fig. 6** The abnormal aggregation kinetics with the transitional process in the shape of a break.

process can be as long as 19 s (Figure 8) and was reliably reproduced in experiments on the same blood sample.

In the experiments focused on the study of the aggregation kinetics in blood samples of normal subjects at different hematocrit ( $H$ ) values we observed the slowing down of the aggregation process ( $T_1$ ) along with the decrease of hematocrit. However no regular dependence of  $T_2$  on  $H$  has been found so far.<sup>24</sup> The study of the disaggregation kinetics showed that the hydrodynamic strength of aggregates determined by the monoexponential algorithm without distinguishing two different parameters of aggregate strength, is inversely proportional to the hematocrit. Variation of hematocrit in the range from 0.2 to 0.8 was performed by diluting the erythrocyte suspension in the autologous blood plasma.

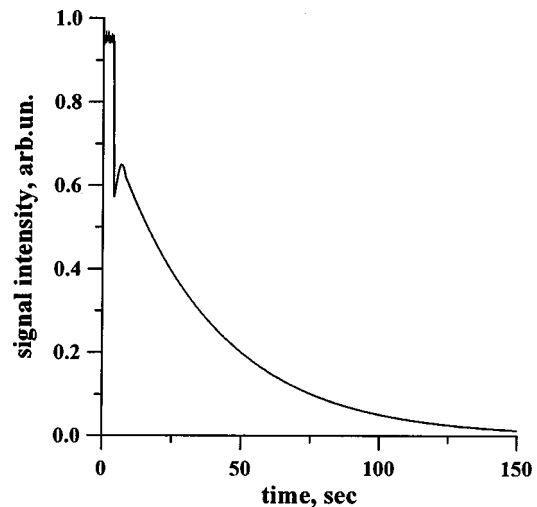


**Fig. 7** The abnormal aggregation kinetics with transitional process in the shape of a cupola-shaped peak.

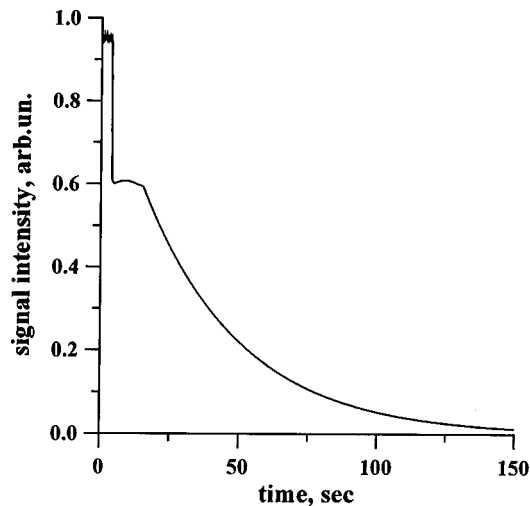


**Fig. 8** The abnormal aggregation kinetics with a delay of aggregation that can be as large as 19 s.

The influence of aging of the blood sample *in vitro* on the aggregation kinetics was also studied.<sup>24</sup> Keeping the blood sample for a long period of time even under thermostabilized conditions at  $t=4-6$  °C induces changes in the erythrocyte shape. Normal discocytes are transformed into echinocytes in 2 days and into spherocytes in 4 days. When the form of RBCs is changed the advantage of the side-by-side aggregation disappears and the aggregation kinetics reduces to one exponent with characteristic time close to  $T_2$  value. The analysis of the  $T_1$  parameter in aged blood samples showed that the increase of the H value results in the decrease of  $T_1$ , which asymptotically approaches a certain value  $T_{1as}=4.0\pm 1.5$  s.<sup>23</sup>

The analysis of the hydrodynamic strength of aggregates showed that there are several types of disaggregation kinetics:

- (i) normal disaggregation kinetics with one index of aggregates strength ( $\beta\sim 30$  s<sup>-1</sup>);
- (ii) two-component process of disaggregation with the strength of large aggregates  $\beta_1$  close to the normal index and the strength of small aggregates  $\beta_2$  increased by 2–4 times (for example in the case of *hereditary glomerulonephritis*  $\beta_1=30\pm 2$  s<sup>-1</sup>, and  $\beta_2=99\pm 3$  s<sup>-1</sup>, and in the case of *Sjogren disease*  $\beta_1=30\pm 2$  s<sup>-1</sup>, and  $\beta_2=132\pm 4$  s<sup>-1</sup>);
- (iii) abnormal two-component disaggregation process with significantly increased strength of large aggregates ( $\beta_1=140\pm 5$  s<sup>-1</sup> and  $\beta_2=81\pm 3$  s<sup>-1</sup>) that we observe only for some samples of blood in the case of *rheumatoid arthritis*.

The case of a two-component disaggregation process in blood of an individual with *pulmonary hypertension*, which is characterized by the low strength

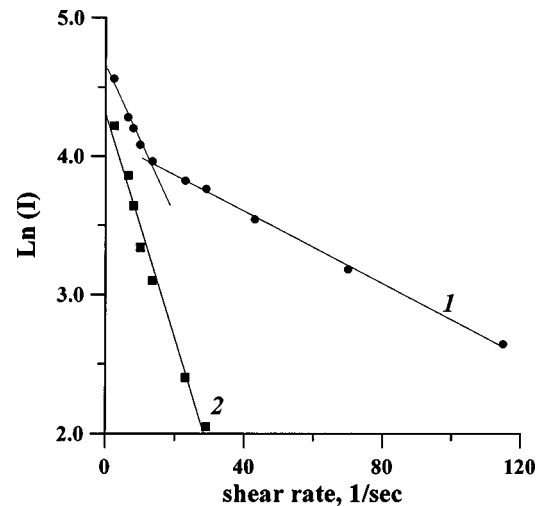


**Fig. 9** Disaggregation kinetics in the case of *pulmonary hypertension* blood (1) and normal blood (2). The corresponding values of aggregates strength are:  $\beta_1=21.2$  s<sup>-1</sup> and  $\beta_2=73.1$  s<sup>-1</sup> (1);  $\beta=24.7$  s<sup>-1</sup> (2).

of large aggregates  $\beta_1$  and the high strength of small aggregates  $\beta_2$ , as well as a one-component process in the case of normal blood are presented in Figure 9.

In some cases no disaggregation was found at low shear rates. Instead a decreased intensity of the backscattered light as a sign of the intensified aggregation process was observed at low shear rates (Figure 10). This effect was characterized quantitatively as the percentage of the complete amplitude of the aggregation and called  $I_{2.5}$ . We have given this parameter a negative sign when the backscattered light intensity increased and a positive sign when the light intensity decreased at the introduction of shear. In the blood of healthy donors the

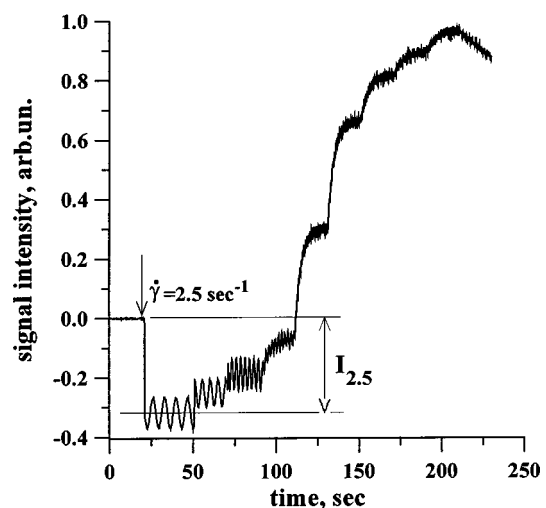


**Fig. 10** The shear-induced aggregation process at the shear rate of  $2.5$  s<sup>-1</sup> under *Sjogren disease*. In this case the parameter  $I_{2.5}$  is positive, as different from Figure 2, and is about 30% lower than the level of total amplitude of aggregation.

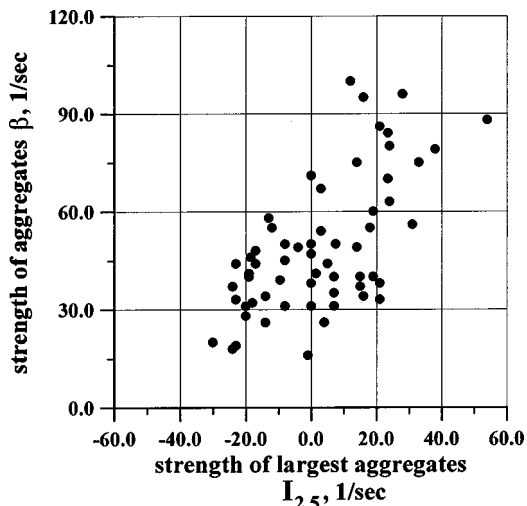


**Fig. 11** The correlation between  $I_{2.5}$  and  $\beta$  in patients with *psoriatic arthritis* ( $r=0.68$ ,  $p<0.05$ ) indicates that shear-induced aggregation is the result of the increased strength of the erythrocyte aggregates. The overall number of points includes the results of multiple measurements performed with blood samples drawn from the same donor on different days.

mean of  $I_{2.5}$  was  $-25.0 \pm 0.8\%$  ( $n=40$ ). Strong and significant correlation ( $r=0.68$ ;  $p<0.05$ ) between  $I_{2.5}$  and  $\beta$  in the case of *psoriatic arthritis* was obtained (Figure 11).<sup>23</sup>

#### 4 DISCUSSION

The values of characteristic times obtained by the aggregometer described above do not coincide with those obtained by other authors with an aggregometer of a different type.<sup>8</sup> The characteristic time of the aggregation process obtained by means of the cone-plate aggregometer was  $3.5 \pm 1.0$  s for normal blood. The big difference results from different construction of the device, namely a different thickness of blood layer ( $\sim 50$   $\mu\text{m}$  in the cone-plate and 1 mm in a Couette type aggregometer) and different orientation of the sedimentation force relative to the gap thickness. In the case of cone-plate design it is directed across the gap and in the Couette flow along it. The sedimentation process, shear forces, and diffusion of the RBCs strongly influence the aggregation kinetics *in vitro*.<sup>26,27</sup> The aggregation of red blood cells combined with the sedimentation due to the gravitational force induces the formation of gradients of concentration that can influence the stability of the blood flow.

Owing to the inhomogeneity of the cohesion properties of erythrocytes the 3-D aggregates, linear ones, and single red blood cells can be simultaneously present in the measured volume. We suppose that at every moment of the aggregation process there is a certain distribution of the sizes of erythrocyte aggregates. The aggregates of the most probable size mostly contribute to the scattering signal registered by the photometer. At the present

time the theory of multiple light scattering in suspensions of aggregating particles is still under development, therefore it is difficult to bring the experimentally registered aggregation kinetics in accordance with the sizes of formed aggregates.

Thus in the case of blood aggregometry it is impossible to strictly distinguish the stages of formation of the aggregates of certain sizes only on the basis of the absolute amount of scattered light. The analysis of the kinetic coefficients is the only reasonable approach possible at the current stage of research.

The original scattering signal curves were processed according to both exponential and hyperbolic algorithms. The analysis of the obtained parameters  $T_1$  and  $\tan \alpha$  for 20 samples of blood shows<sup>22</sup> that the dependence between these indices is hyperbolic with the constant  $(T_1 \cdot \tan \alpha) = 5.95 \pm 0.25$ . This means the similarity of both algorithms but the exponential method gives more detailed information about the different stages of the aggregation process.

The instant aggregation process observed in the case of *inherited hyperlipemia* (Figures 6–8) corresponds, as we suppose, to the formation of primary red cell aggregates. Basically these are pairs of erythrocytes and their formation is vastly induced both by the remaining convection, and by that circumstance that pairs are formed due to the rotation of cells already having contact. Following this process a delay of aggregation is difficult to explain, but this effect can be interpreted in favor of theories of long-range interaction between erythrocytes.<sup>28</sup> In a suspension with a small amount of macromolecules after forming the pair aggregates (the instant component) a certain amount of time is necessary for creating a macromolecular structure in erythrocyte "atmosphere," in order to overcome the formed plasma layer and to join erythrocytes in rouleaux. The appearance of the cupola-shaped peak on the aggregation kinetics can be explained by changes in the orientation of pair aggregates after their forming.

The study of disaggregation of erythrocyte aggregates in shear flow has shown that this process is different not only for different diseases but for different samples of blood under the same pathology and for different hematocrit values. Usually the value of  $\beta_1$  was lower than  $\beta_2$ . This may be a result of the homogeneity of cohesion properties of the erythrocytes manifested by the successive destruction primarily of clumps or network and then by the destruction of the rouleaux oriented along the flow. The effect of shear stress is low on linear aggregates and complete disaggregation can only occur at high shear rates.

The effect of intensified erythrocyte aggregation induced by low shear rates was observed even in the blood of healthy donors. Copley et al.<sup>29</sup> found this effect in whole blood at a shear rate of  $\dot{\gamma}$

$=0.1 \text{ s}^{-1}$ . Chen et al.<sup>30</sup> registered an intensified aggregation process in whole blood at low hematocrit by adding 0.5% Dextran DX-500. The phenomenon of the shear-induced aggregation (hyperaggregation) was caused by the formation of pathological aggregates with high strength.

Strong and significant correlation ( $r=0.68$ ;  $p < 0.05$ ) between  $I_{2.5}$  and  $\beta$  in the case of *psoriatic arthritis* indicates that the effect of the shear-induced aggregation is the result of the increased strength of the erythrocyte aggregates. At normal hematocrit and positive  $I_{2.5}$  the process of spontaneous aggregation has been completed when the 3-D network of the linear erythrocyte aggregates had been formed. The shear stress causes the destruction of this network and spheroid-like aggregates are then formed. This process can be observed when shear stress at the shear rate of  $2.5 \text{ s}^{-1}$  is lower than the strength of the spheroid-like erythrocyte aggregates.

The analysis of H dependencies of  $T_1$  for normal blood and *hereditary glomerulonephritis* allowed us to conclude that this parameter is proportional to  $H^{-2}$ , the coefficients requiring additional measurements.<sup>24</sup> The data obtained on the disaggregation kinetics showed that the strength of RBC aggregates is inversely proportional to the hematocrit. Such dependence is explained by the fact that the decrease in the concentration of erythrocytes results in the increase of the quantity of plasma proteins (fibrinogen, globulins, etc.) inducing the aggregation, per one RBC.<sup>24</sup> At low H values the shear-induced aggregation and sedimentation processes are manifested simultaneously. Thus the aggregation and disaggregation parameters measured by the backscattering technique are sensitive to the hematocrit changes. So it is important that the experiments be carried out with blood samples at one fixed value of hematocrit, e.g.,  $H=0.4$ .

The system of aggregation parameters presented and discussed in this paper makes possible a quantitative estimation of processes of linear erythrocyte aggregates and 3-D aggregates (clumps) formation. In the case of hyperaggregation syndrome it is sometimes possible to evaluate separately the strength of the largest aggregates ( $I_{2.5}$ ) as well as that of large ( $\beta_1$ ) and linear ( $\beta_2$ ) red blood cells aggregates. So we believe that the combination of aggregation and disaggregation parameters can be considered as a diagnostically meaningful pattern of hemorheological pathology.

## ACKNOWLEDGMENTS

This work was supported in part by Grant No. 96-15-97782 for leading Russian scientific schools (biological and medical sciences).

## REFERENCES

1. H. Schmid-Schönbein, H. Malotta, and F. Striesow, "Erythrocyte aggregation: causes, consequence and methods of assessment", *J. Netherlands Soc. Clin. Chem.* **15**, 88-97 (1990).
2. H. Schmid-Schönbein, H. Reiger, and G. Gallasch, "Pathological red cell aggregation," *Recent Advances in Clinical Microcircular Res.*, Part 2, No. 16, pp. 484-489, Basel (1977).
3. E. A. Evans, "Minimum energy analysis of membrane deformation applied to pipet aspiration and surface adhesion of red blood cells," *Biophys. J.* **30**, 265-284 (1980).
4. E. Evans and K. Buxbaum, "Affinity of red cell membrane for particle surfaces measured by the extent of encapsulation," *Biophys. J.* **34**, 1-12 (1981).
5. A. Dognon, L. Loeper, and E. Housset, "Etude optique de l'aggregation reversible des hematies," *C. R. Sci. Soc. Biol.* **143**, 769-771 (1949).
6. A. Dognon and P. Suquet, "Facteur de reflexion diffuse des suspensions de particules colorees," *J. Chem. Phys.* **10**, 815-820 (1957).
7. H. Schmid-Schönbein, K. A. Kline, L. Heinich, E. Volger, and T. Fischer, "Microrheology and light transmission of blood," *Pflugers Arch. Ges. Physiol. Menschen Tiere* **333**(2), 140-155 (1972).
8. H. Schmid-Schönbein, K. A. Kline, and E. Volger, "Velocity of red cell aggregation (RCA): photometric determination of the half-time and aggregation constant," *Bibl. Anat.* **13**, 91-92 (1975).
9. L. Dintenfass, A. Wellard, and H. Jedrzezyk, "Photographic, stereological, and statistical methods in evaluation of aggregation of red cells in disease. Part 1: Kinetics of aggregation," *Biorheology* **19**(4), 567-577 (1982).
10. V. A. Levtov, S. A. Regirer, and N. Kh. Shadrina, "On red blood cell aggregation," in *Contemporary Problems of Biomechanics*, G. G. Chernyi and S. A. Regirer, Eds., pp. 55-74, Mir Publishers; CRC Press, Boca Raton (1990).
11. T. L. Fabry, "Mechanism of erythrocyte aggregation and sedimentation," *Blood* **70**(5), 1572-1576 (1987).
12. J. F. Stoltz and M. Donner, "Erythrocyte aggregation: experimental approaches and clinical implication," *Int. Angiol.* **6**(2), 193-201 (1987).
13. M. R. Hardeman, P. T. Goedhart, L. G. G. Dobbe, and K. P. Lettinga, "Laser-assisted optical rotational cell analyzer (L.O.R.C.A.); I. A new instrument for measurement of various structural hemorheological parameters," *Clin. Hemorheol.* **14**(4), 605-618 (1994).
14. M. Donner, M. Siadat, and J. F. Stoltz, "Erythrocyte aggregation: Approach by light scattering determination," *Biorheology* **25**, 367-375 (1988).
15. A. H. Gandjbakhche, P. Mills, and P. Snabre, "Light-scattering technique for the study of orientation and deformation of red blood cells in a concentrated suspension," *Appl. Opt.* **30**(6), 1070-1078 (1994).
16. A. V. Priezzhev, O. M. Ryaboshapka, and N. N. Firsov, "Light scattering anisotropy in the diagnostics of structural and orientational effects of RBC's in whole blood in Couette flow," in *Optical Diagnostics of Living Cells and Biofluids*, T. Asakura, D. Farkas, R. C. Leif, A. V. Priezzhev, and B. J. Tromberg, Eds., *Proc. SPIE* **2678**, 342-345 (1996).
17. A. V. Priezzhev, S. G. Khatsevich, and V. V. Lopatin, "Asymmetry of light backscattering from Couette flow of RBC suspensions: Application for biomonitoring of blood samples," Paper #3567-40 presented at BiOS-Europe'98, *Proc. SPIE* **3567** (to be published).
18. N. N. Firsov, A. V. Priezzhev and O. M. Ryaboshapka, "Aggregation properties of erythrocytes of whole blood under shear stress by backscattering nephelometry," in *Static and Dynamic Light Scattering in Medicine and Biology*, R. J. Nossal, R. Pecora, and A. V. Priezzhev, Eds., *Proc. SPIE* **1984**, 283-290 (1993).
19. N. N. Firsov, A. V. Priezzhev, and O. M. Ryaboshapka, "Aggregation and disaggregation kinetics of erythrocytes in whole blood under low-energy laser irradiation," in *Medical Applications of Lasers*, K. Atsumi, C. Borst, F. W. Cross et al., Eds., *Proc. SPIE* **2086**, 365-370 (1993).
20. A. V. Priezzhev, N. N. Firsov, E. F. Stranadko, O. M. Ryaboshapka, T. V. Chichuk, and O. V. Suschinskaya, "Aggregation and hemolysis of erythrocytes under photodynamic therapy," in *Photochemotherapy: Photodynamic Therapy and*



- Other Modalities. II*, S. B. Brown, B. Ehrenberg, and J. Mba, Eds., *Proc. SPIE* **2924**, 212–218 (1996).
21. N. N. Firsov, A. V. Priezzhev, and O. M. Ryaboshapka, "Study of erythrocytes aggregation kinetics in shear flow in vitro by light scattering technique," in *Optical Methods of Biomedical Diagnostics and Therapy*, V. V. Tuchin, Ed., *Proc. SPIE* **1981**, 17–25 (1993).
  22. A. V. Priezzhev, N. N. Firsov, O. M. Ryaboshapka, and M. G. Vyshlova, "Aggregation kinetics of erythrocytes in whole blood: comparison of data processing algorithms," in *Optical Diagnostics of Biological Fluids and Advanced Techniques in Analytical Cytology*, A. V. Priezzhev, T. Asakura, and P. C. Leif, Eds., *Proc. SPIE* **2982**, 220–225 (1997).
  23. N. N. Firsov, A. Bjelle, T. V. Korotaeva, A. V. Priezzhev, and O. M. Ryaboshapka, "Clinical application of the measurement of spontaneous erythrocyte aggregation and disaggregation. A pilot study," *Clin. Hemorheol.* **18**(2-3), 87–97 (1998).
  24. N. N. Firsov, A. V. Priezzhev, O. M. Ryaboshapka, I. V. Sirko, and M. A. Vyshlova, "Dependences of erythrocyte aggregation and disaggregation parameters of suspension hematocrit: study by backscattering nephelometry," in *Laser Applications in Life Sciences*, P. A. Apanasevich, N. I. Koroteev, S.G. Kruglik, and V. N. Zadkov, Eds., *Proc. SPIE* **2370**, 393–399 (1995).
  25. P. Snabre, M. Bitbol, and P. Mills, "Cell disaggregation behavior in shear flow," *Biophys. J.* **51**, 795–807 (1987).
  26. E. S. Losev, N. V. Netrebko and I. V. Orlova, "Gravitational sedimentation of aggregating particles in shear flow," *Fluid Dyn. (USSR)* **24**(2), 242–245 (1989).
  27. E. S. Losev, N. V. Netrebko, S. A. Regirer, A. S. Stepanyan, and N. N. Firsov, "Interaction between gravitational sedimentation and shear diffusion in suspension moving in rotation viscosimeter gap," *Fluid Dyn. (USSR)* **25**(5), 685–691 (1990).
  28. L. Dintenfass, *Microvasc. Res.* **11**, 325–327 (1976).
  29. A. L. Copley, C. R. Huang, R. G. King, and S. Oka, "Erythrocyte sedimentation of human blood at varying shear rates," *Biorheology* **13**, 281–286 (1976).
  30. S. Chen, G. Barstein, B. Gavish, Y. Mahler, and S. Yedgar, "Monitoring of red blood cell aggregability in a flow-chamber by computerized image analysis," *Clin. Hemorheol.* **14**, 497–508 (1994).